



# Assessment of flux and energy buildup factors in shielding of some gamma sources used for industrial radiography

Rahim Khabaz<sup>a</sup>

Department of Physics, Faculty of Sciences, Golestan University, 49138-15739 Gorgan, Iran

Received: 9 July 2021 / Accepted: 2 March 2022

© The Author(s), under exclusive licence to Società Italiana di Fisica and Springer-Verlag GmbH Germany, part of Springer Nature 2022

**Abstract** In radiation shielding, health physics, knowing buildup factors of various materials is necessary. This paper attempts to perform some Monte Carlo simulations with the most recent cross section data to calculate the buildup factors associated with flux and energy of several gamma-ray sources ( $^{60}\text{Co}$ ,  $^{137}\text{Cs}$ ,  $^{192}\text{Ir}$ ,  $^{75}\text{Se}$  and  $^{169}\text{Yb}$ ) that are commonly employed in industrial radiography by considering radiation shielding materials: Al, concrete, Fe, Sn, Pb, W and U. Linear attenuation coefficient and flux buildup factors were compared with the coefficient measured with a CsI(Tl)-based  $\gamma$ -ray spectrometer for  $^{60}\text{Co}$  and  $^{137}\text{Cs}$  sources. During this work, the energy buildup factors were fitted based on Berger's formula and the related coefficients were determined for each radionuclide source-shielding material configuration.

## 1 Introduction

Industrial radiography is a nondestructive method which allows testing components for flaws without interfering with their usefulness. This technique is one of the inspection methods that are commonly employed for quality control of manufactured products and monitoring their performance in service, in industry [1, 2].

Gamma-rays from most radioactive sources have a great power of penetrating, which makes them valuable, especially when large thicknesses or high-density specimens, beyond the range of generally available X-ray equipment, are involved. The radioisotopes that are commonly used include  $^{60}\text{Co}$ ,  $^{137}\text{Cs}$ ,  $^{192}\text{Ir}$ ,  $^{75}\text{Se}$  and  $^{169}\text{Yb}$  [3]. The mean energy of these sources is 1.252, 0.662, 0.375, 0.218 and 0.145 MeV, respectively [4]. The sources can be classified according to the energy they emit: high ( $^{60}\text{Co}$ ), medium ( $^{137}\text{Cs}$  and  $^{192}\text{Ir}$ ) and low energy ( $^{75}\text{Se}$  and  $^{169}\text{Yb}$ ). In other words, the  $^{60}\text{Co}$  is most energetic source and for shielding need thicker layer of the shield, while protection of the  $^{169}\text{Yb}$  is more comfortable and can be done with similar thinner layers. Furthermore, the materials with higher atomic number have greater value of photoelectric cross section and then can have better shielding against radiation.

People whose jobs relate to radiation, e.g., radiographers, can be affected by ionizing radiation. The received radiation dose depends on different parameters and conditions, for example, distance, time, working procedure and shielding. Therefore, it is crucial for higher level personnel to continuously evaluate the extent and intensity of the radiation imposed on each radiographer employee to guarantee employee's safety. The most important issue for use of such gamma sources in the industrial radiography is proper shielding [5].

International atomic energy agency (IAEA) has recommended that the shielding should be such that in controlled areas the dose equivalent be less than 5 mSv/year and for uncontrolled areas less than 1 mSv/year [6]. The ICRP has proposed limiting radiation exposure dose for occupational radiation worker is a mean of 20 mSv/year over five years and 1 mSv/year for the public [7]. The ICRP subscribes the general philosophy of not only keeping exposures under the dose limits, but also preservation all exposure levels "as low as reasonable achievable" (ALARA).

One of the interactions of photons with matter is the Compton scattering in which secondary scattered photons are produced. The generation of these secondary radiations impacts the entire process of penetration and diffusion of gamma-rays, since secondary radiations can reach the detector [8, 9]. When secondary gamma-rays accumulate during the attenuation process, a correction factor arises which is known as "buildup factor" [10, 11]. Furthermore, the buildup factor is defined as the parameter which arises as an outcome from multiple gamma-ray photons scattering within a material due to large penetration depth of material and a consequence of divergence or broad beam of gamma-ray photon [12].

Knowing the dose of photons is important in radiation protection, radiation hazards, external exposure, industrial applications and other cases where there are photons. Concentrating on the protection of people, one may want to know, at any location where people might be working or living, or exposed to photons, the exposure and dose rate of the gamma. The buildup factor is the key part for the occupational exposure evaluation, which is the basis for many advanced dose evaluation methods [13–18].

<sup>a</sup> emails: [r.khabaz@gu.ac.ir](mailto:r.khabaz@gu.ac.ir); [ra\\_khabaz@yahoo.com](mailto:ra_khabaz@yahoo.com) (corresponding author)

Much progress has been made over the years about calculating the buildup factor in various media and for a wide range of incident photon energy and penetration depth. In principle, the buildup factors can be investigated experimentally [19, 20]. Buildup factors are usually calculated theoretically by the solving the photon transport equation [21, 22]. Nowadays, with developed gamma transport and to the well-evaluated accurate values of attenuating coefficients and cross sections, the various buildup factors can be calculated through the Monte Carlo method [13, 23–25]. Moreover, this approach provides convenient consideration of the gamma source energy spectrum and effect of the employed materials.

In previous works, the buildup factors have been obtained for monoenergetic photons [26–28]. In this study, the flux and energy buildup factors for some gamma sources used for industrial radiography, i.e., <sup>60</sup>Co, <sup>137</sup>Cs, <sup>192</sup>Ir, <sup>75</sup>Se and <sup>169</sup>Yb are calculated by Monte Carlo transport code MCNPX, for seven shields. These sources, except <sup>137</sup>Cs, emit more than one gamma energy.

## 2 Materials and methods

For penetration data, a combination of exponential linear attenuation coefficients, the inverse square law and the assumption of buildup factors to account for single and multiple scattering events were considered [29]. In gamma-ray transmission through a material, the photon flux reached the detector ( $\Phi$ ) at  $r$  distance from a point source follows:

$$\Phi = B(\mu r, E) \Phi_0 e^{-\mu r} \tag{1}$$

where  $\Phi_0$  is the flux reached the detector in the lack of the material (i.e., a vacuum between source and detector),  $\mu$  is the linear attenuation coefficient for the source photons, and  $B(\mu r, E)$  represents the buildup factor which scores for photons scattered by the shield into the detector. The flux reached the detector ( $\Phi$ ) may be broken up into two parts, contributed by the uncollided or unscattered ( $\Phi_u$ ) and collided or scattered ( $\Phi_s$ ) photons:

$$\Phi = \Phi_u + \Phi_s \tag{2}$$

The buildup factor can include several types: number, energy deposited, exposure and flux buildup factor. The flux buildup factor ( $B_F$ ) of an isotropic point source, emitting one photon per second, placed in the center of a spherical medium with a radius of  $r$  can be defined as the ratio of detector record due to both unscattered and scattered radiation over the detector record because of unscattered radiation only:

$$B_F(\mu r, E) = \frac{\Phi}{\Phi_u} = \frac{\Phi}{\Phi_0 e^{-\mu r}} = 4\pi r^2 e^{\mu r} \Phi \tag{3}$$

Similarly, energy buildup factor ( $B_E$ ) can be obtained from:

$$\begin{aligned} B_E(\mu r, E) &= \frac{\int_0^\infty \Phi(r, E) E dE}{\int_0^\infty \Phi_u(r, E) E dE} \simeq \frac{\sum_j \Phi_j(r, E) E_j}{\sum_i \Phi_{u_i}(r, E) E_i} \\ &= (4\pi r^2 e^{\mu r}) \frac{\sum_j \Phi_j(r, E) E_j}{\sum_i f_i E_i} \end{aligned} \tag{4}$$

where  $f_i$  refers to the intensity of emitted photons by source having energy  $E_i$  [11, 12]. Generally, buildup factor depends on photons' energies, source geometry (parallel beam or point isotropic source) and geometry of the attenuating medium (finite, infinite, slab, etc.).

This study was carried out on the buildup factors of five radionuclide gamma sources, i.e., <sup>60</sup>Co, <sup>137</sup>Cs, <sup>192</sup>Ir, <sup>75</sup>Se and <sup>169</sup>Yb for seven shields: Al, concrete, Fe, Sn, Pb, W and U.

### 2.1 Monte Carlo calculations

Calculations were performed with the MCNPX code [30] and cross sections were obtained from the latest cross section library MCPLIB02 [31]. The elemental composition and the density of shielding materials were obtained from ‘‘Compendium of Material Composition Data for Radiation Transport Modeling’’ [32]. The elemental composition of concrete was 51.260% O, 36.036% Si, 5.791% Ca, 3.555% Al, 1.527% Na, 1.378% Fe and 0.453% H, whose density was 2.25 g/cm<sup>3</sup>. At the first step, calculating the linear attenuation ( $\mu(E)$ ) was performed for each configuration of the source shield. To obtain this parameter, a slab of each shield with 1 cm thickness was exposed to each plane gamma source, while emitting a parallel beam (Fig. 1). Then, parallel photons ( $I$ ) are tallied on the slab's exit surface with a current tally (F1) associated with a cosine card.

**Fig. 1** Simulated setup for obtaining the linear attenuation coefficient

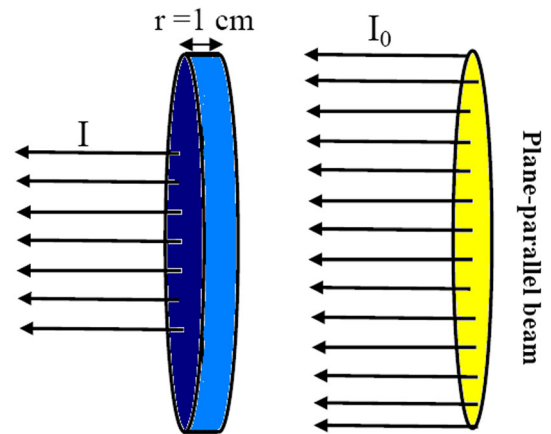
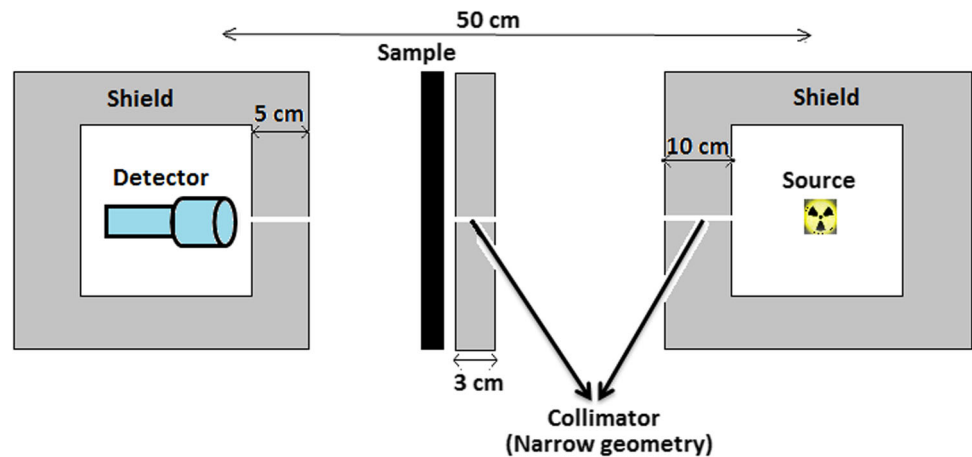


**Fig. 2** Experimental setup for measuring the linear attenuation coefficient



In this case, the buildup factor of Eq. (1) is unit, and also outputs of MCNPX are normalized per photon emitted by the source (per history); then, the  $\mu(cm^{-1})$  for 1 cm thickness of each shield can be calculated based on:

$$\mu(Z, E) = -\ln(I) \tag{5}$$

Finally, using the obtained  $\mu(E)$  values, the flux and energy buildup factors of these radionuclide gamma sources were calculated using Eqs. (3) and (4), respectively.

In computing the shield thickness, it has been assumed that the radiation source is a point source. It is possible to treat a line source or other large radiation source as a point source, if the distance from the source is more than twice its maximum dimension. The deviation induced in the results due to above assumption is not more than 4% [33].

The simulated geometry contains an isotropic point source at the center of a sphere. For each source, calculations were made for penetration depth up to 10 mean free paths (mfp). To achieve buildup factor values, the surface flux tally (F2) in the MCNPX code was used for calculation of total flux ( $\Phi$ ) and the group flux in the  $j^{th}$  energy bin ( $\Phi_j$ ); then by Eqs. (3) and (4), buildup factors of flux and energy were determined, respectively. All MCNPX calculations were done up to suitable histories ( $10^8$ ) which give an admissible relative statistical error ( $\leq 0.5\%$ ).

### 2.2 Measurements

Using the  $^{137}\text{Cs}$  and  $^{60}\text{Co}$  sources in a lead shield with a 5 mm-diameter collimator, several transmission experiments were carried out. At first, the measurement was for obtaining the linear attenuation coefficient of lead and iron irradiated by  $^{137}\text{Cs}$  and  $^{60}\text{Co}$  point radioactive sources (370 MBq). This experiment consists of a measuring head, including a source container for each source, and a CsI(Tl) scintillation detector ( $\varnothing 3.81\text{ cm} \times 3.81\text{ cm}$ ) sited in the shield. The sample layers of lead and iron with thicknesses of 1.0 cm, and sizes of  $20 \times 20\text{ cm}^2$  were placed between the source and the detector. The distance between the detector and the source was 50 cm.

Since for obtaining the  $\mu$  value based on the Beer–Lambert law the incident and transmitted photons must be parallel, the gamma-ray beam transmission was collimated using a narrow geometry array. The general configuration of the geometry is shown in Fig. 2.

**Fig. 3** Schematic view of the experimental setup for measurement of buildup factor with collimator

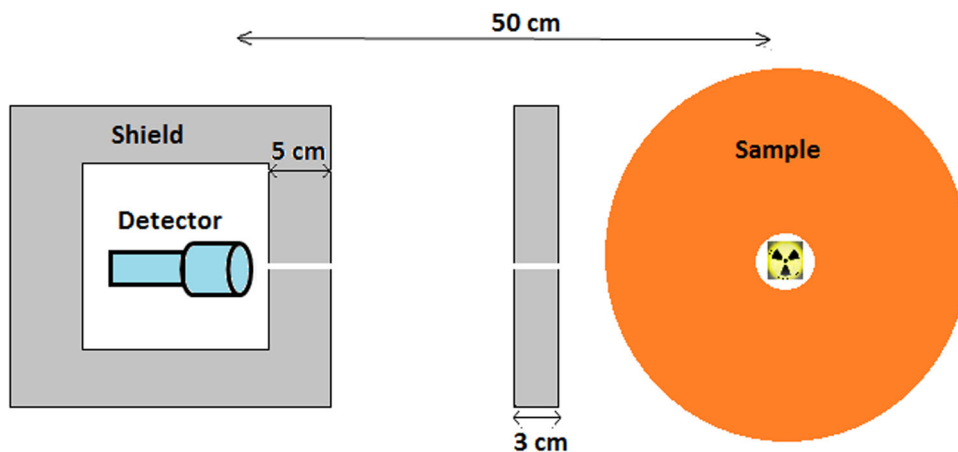


**Table 1** Calculated linear attenuation coefficient ( $\mu(E)$ ) by MCNPX

	$^{60}\text{Co}$		$^{137}\text{Cs}$		$^{192}\text{Ir}$		$^{75}\text{Se}$		$^{169}\text{Yb}$	
	$\mu$ ( $\text{cm}^{-1}$ )	Error	$\mu$ ( $\text{cm}^{-1}$ )	Error	$\mu$ ( $\text{cm}^{-1}$ )	Error	$\mu$ ( $\text{cm}^{-1}$ )	Error	$\mu$ ( $\text{cm}^{-1}$ )	Error
Al	0.1484	0.0001	0.2018	0.0001	0.2611	0.0002	0.3333	0.0002	0.4476	0.0001
Concrete	0.1283	0.0001	0.1746	0.0001	0.2256	0.0002	0.2874	0.0002	0.3840	0.0002
Fe	0.4198	0.0003	0.5779	0.0003	0.7840	0.0003	1.2049	0.0005	1.7178	0.0002
Sn	0.3699	0.0003	0.5506	0.0003	0.9685	0.0004	1.8898	0.0007	2.9061	0.0004
Pb	0.6580	0.0002	1.2290	0.0002	2.7287	0.0004	5.0059	0.0012	10.2524	0.0008
W	1.0594	0.0003	1.8461	0.0002	3.5801	0.0006	7.6604	0.0007	13.7584	0.0008
U	1.2090	0.0007	2.4472	0.0003	4.6485	0.0010	10.4317	0.0014	17.7819	0.0014

In the following, the flux buildup factor is measured based on the relation between the incoming gamma-rays and gamma-rays passing through the spherical materials. In these experiments, the  $^{137}\text{Cs}$  and  $^{60}\text{Co}$  sources are placed at the center of lead and iron spheres. For  $^{60}\text{Co}$  source, radii of the iron sphere were 7.15 and 11.91 cm and lead sphere had radii of 4.56 and 7.60 cm. For measurement with  $^{137}\text{Cs}$  source, the iron sphere with radii of 5.19 and 8.65 cm and lead sphere with radii of 2.44 and 4.07 cm were used. These selected radii are equal to 3 and 5 mfp of each source-shield configuration. The CsI(Tl) detector was placed at a 50 cm distance from the center of sphere (gamma source). For each sphere, the buildup factor was measured based on two statuses: with collimator between sphere and detector and without collimator. A schematic view of geometry used for buildup factor measurement with collimator is shown in Fig. 3.

### 3 Results and discussion

The  $\mu(E)$  coefficient for each configuration of the source shield was calculated according to Monte Carlo simulation, in this work, and is presented in Table 1.

Using the results of Table 1, the flux and energy buildup factors of gamma sources used for industrial radiography, i.e.,  $^{60}\text{Co}$ ,  $^{137}\text{Cs}$ ,  $^{192}\text{Ir}$ ,  $^{75}\text{Se}$  and  $^{169}\text{Yb}$ , positioned at the center of seven spherical shields (Al, concrete, Fe, Sn, Pb, W and U) with different radius from 1 to 10 mfp, are calculated. The findings of flux buildup factors are illustrated in Figs. 4, 5, 6, 7 and 8 for  $^{60}\text{Co}$ ,  $^{137}\text{Cs}$ ,  $^{192}\text{Ir}$ ,  $^{75}\text{Se}$  and  $^{169}\text{Yb}$  sources, respectively.

The obtained results show that this factor increases with the width of the shield for each source. This is because that the increase in the penetration depth increases the interaction of gamma radiation photons with material resulting in generating a lot of low energy photons due to Compton scattering process. The values of this factor for aluminum and concrete are very close to each other. By comparing the results, it is obvious that the buildup factor for each shield increases by decreasing the mean energy of gamma source, excluding at penetration depths 1 and 2 mfp; in the way, the  $^{169}\text{Yb}$  and  $^{60}\text{Co}$  have the highest and lowest amount of this factor for all materials. For  $^{169}\text{Yb}$ , the flux buildup factors are found to be in the range 0.64–384.79 at penetration depths 1–10 mfp. The flux buildup factors of  $^{60}\text{Co}$  source varied in the range 1.56–43.78. It may be seen that the buildup factor for each source increases with decrease in the atomic number of shield material; however, the aluminum and uranium have the maximum and minimum values of buildup factor among the others, respectively. The reason is that Compton scattering is the most dominant type of scattering for low-Z materials, especially for gamma-rays with medium energy. The buildup factors for uranium exposed to the  $^{137}\text{Cs}$  have roughly

**Fig. 4** Flux buildup factors for different spherical shields exposed to  $^{60}\text{Co}$  source

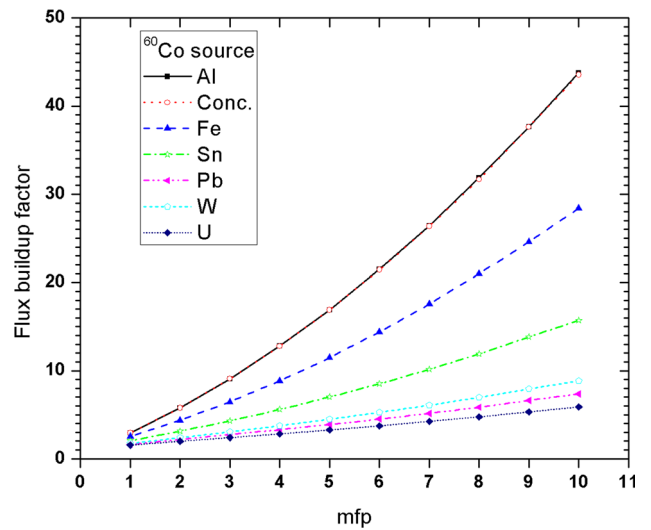


**Fig. 5** Flux buildup factors for different spherical shields exposed to  $^{137}\text{Cs}$  source

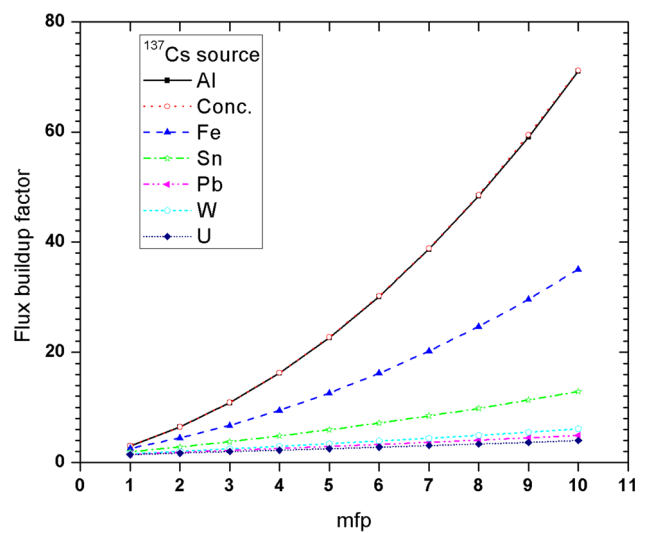
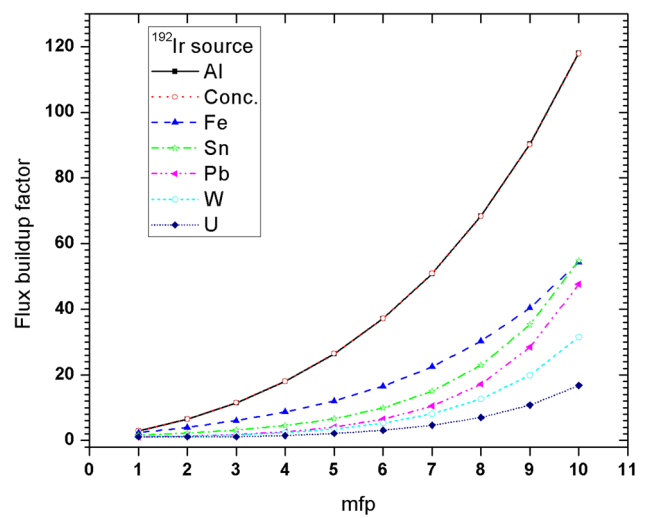


**Fig. 6** Flux buildup factors for different spherical shields exposed to  $^{192}\text{Ir}$  source



slight changes from 1.40–3.99 at penetration depths. The small buildup factors are also due to the dominance of photoelectric effect which results in the complete removal of low energy photons thereby not allowing them to buildup in the medium. Thus, uranium, lead and tungsten (with the high atomic number) show the lowest buildup factors.

**Fig. 7** Flux buildup factors for different spherical shields exposed to <sup>75</sup>Se source

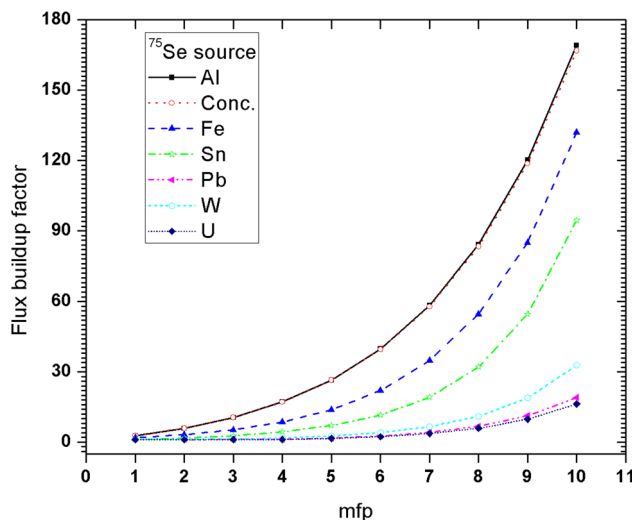
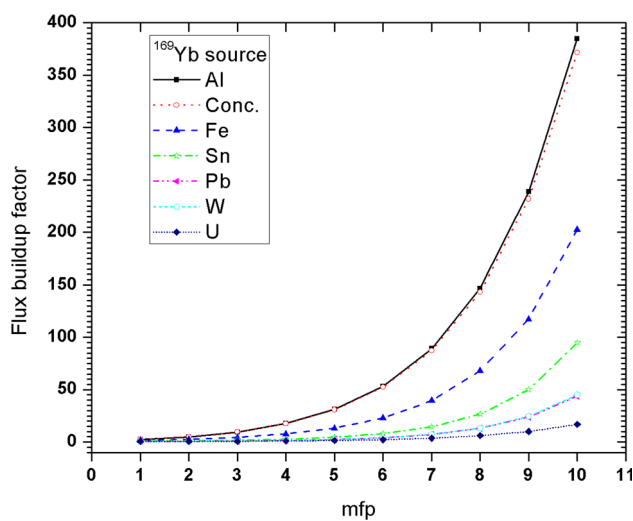


**Fig. 8** Flux buildup factors for different spherical shields exposed to <sup>169</sup>Yb source



Furthermore, the calculated energy buildup factors are listed in Tables 2, 3, 4, 5 and 6 associated with relative statistical errors for different sources and shields.

For identical source and similar penetration depth of each shield, the values of energy buildup factors are lower than the amount of flux buildup factor.

There are several algebraic expressions that have been used to represent energy buildup factor. Among the most popular is an expression referred to as Berger’s form of the buildup factor, given by:

$$B(\mu r, E) = 1 + a(E) \mu r e^{b(E)\mu r} \tag{6}$$

where  $a(E)$  and  $b(E)$  are attributed to constant coefficients of the specific energy and shield material [34].

The results for energy buildup factor were fitted based on Eq. (6), and coefficients  $a(E)$  and  $b(E)$  of the  $B_E$  were calculated for various gamma sources and shields. An example fitting to get coefficients  $a(E)$  and  $b(E)$  is shown in Fig. 9 for <sup>192</sup>Ir source inside the lead shield.

The quantified values of coefficients  $a(E)$  and  $b(E)$  are listed in Table 7.

The Berger fitting computational method was compared with MCNPX for energy buildup factor in the all shields. Figure 10 shows that the energy buildup factors in various materials obtained by Berger fitting and MCNPX at different penetration depths are in very good agreement.

The absolute deviation in MCNPX results of energy buildup factor by Berger fitting is in the range 0.20–4.22%, 0.24–4.87%, 0.005–4.12%, 0.009–1.79% and 0.022–1.71% for <sup>60</sup>Co, <sup>137</sup>Cs, <sup>192</sup>Ir, <sup>75</sup>Se and <sup>169</sup>Yb, respectively. The comparative analysis of energy buildup factor for photon sources at various penetration depths shows that the Berger fitting method can be employed safely for computation of buildup factors of the selected materials.

**Table 2** Energy buildup factors for different spherical shields exposed to <sup>60</sup>Co source with relative error

mfp(μr)	Al		Concrete		Fe		Sn		Pb		W		U	
	B <sub>E</sub>	Rel. Er	B <sub>E</sub>	Rel. Er	B <sub>E</sub>	Rel. Er	B <sub>E</sub>	Rel. Er	B <sub>E</sub>	Rel. Er	B <sub>E</sub>	Rel. Er	B <sub>E</sub>	Rel. Er
1	1.7318	0.0001	1.7310	0.0001	1.6861	0.0001	1.5794	0.0001	1.4128	0.0001	1.4573	0.0001	1.3586	0.0001
2	2.6567	0.0001	2.6542	0.0001	2.4992	0.0001	2.2076	0.0001	1.7995	0.0002	1.9024	0.0002	1.6786	0.0002
3	3.7246	0.0002	3.7192	0.0002	3.4298	0.0002	2.8977	0.0002	2.1937	0.0003	2.3639	0.0003	1.9975	0.0003
4	4.9279	0.0003	4.9165	0.0003	4.4731	0.0003	3.6505	0.0003	2.6050	0.0004	2.8496	0.0004	2.3271	0.0005
5	6.2624	0.0004	6.2439	0.0004	5.6279	0.0005	4.4688	0.0005	3.0408	0.0007	3.3663	0.0006	2.6732	0.0007
6	7.7315	0.0006	7.6956	0.0006	6.8949	0.0007	5.3531	0.0008	3.5052	0.0010	3.9164	0.0010	3.0460	0.0011
7	9.3208	0.0009	9.2705	0.0009	8.2633	0.0010	6.3112	0.0012	4.0045	0.0016	4.5072	0.0015	3.4466	0.0017
8	11.0422	0.0014	10.9729	0.0014	9.7396	0.0016	7.3340	0.0019	4.5360	0.0025	5.1349	0.0023	3.8675	0.0027
9	12.8804	0.0022	12.8160	0.0022	11.2999	0.0024	8.4458	0.0029	5.0989	0.0038	5.7996	0.0036	4.3176	0.0042
10	14.8348	0.0033	14.7366	0.0034	12.9139	0.0037	9.5753	0.0044	5.6606	0.0060	6.4899	0.0055	4.7787	0.0066

**Table 3** Energy buildup factors for different spherical shields exposed to <sup>137</sup>Cs source with relative error

mfp(μr)	Al		Concrete		Fe		Sn		Pb		W		U	
	B <sub>E</sub>	Rel. Er	B <sub>E</sub>	Rel. Er	B <sub>E</sub>	Rel. Er	B <sub>E</sub>	Rel. Er	B <sub>E</sub>	Rel. Er	B <sub>E</sub>	Rel. Er	B <sub>E</sub>	Rel. Er
1	1.9340	0.0001	1.9341	0.0001	1.8358	0.0001	1.6038	0.0001	1.3423	0.0001	1.4018	0.0001	1.2846	0.0001
2	3.2613	0.0001	3.2622	0.0001	2.8722	0.0001	2.2334	0.0001	1.6388	0.0002	1.7655	0.0002	1.5207	0.0002
3	4.9243	0.0002	4.9270	0.0002	4.1098	0.0002	2.9172	0.0002	1.9301	0.0003	2.1306	0.0003	1.7484	0.0003
4	6.9169	0.0002	6.9209	0.0002	5.5541	0.0003	3.6588	0.0004	2.2233	0.0005	2.5050	0.0005	1.9753	0.0005
5	9.2529	0.0004	9.2575	0.0004	7.2137	0.0004	4.4620	0.0006	2.5271	0.0008	2.8912	0.0007	2.2096	0.0008
6	11.9332	0.0005	11.9396	0.0005	9.0901	0.0006	5.3259	0.0009	2.8396	0.0012	3.2951	0.0011	2.4480	0.0013
7	14.9674	0.0008	14.9796	0.0008	11.1742	0.0010	6.2474	0.0013	3.1665	0.0019	3.7212	0.0017	2.6972	0.0020
8	18.3542	0.0012	18.3784	0.0012	13.4631	0.0014	7.2419	0.0020	3.5062	0.0029	4.1597	0.0027	2.9491	0.0032
9	22.0839	0.0018	22.1565	0.0018	16.0030	0.0022	8.2918	0.0031	3.8580	0.0046	4.6298	0.0042	3.1859	0.0051
10	26.1922	0.0027	26.1970	0.0027	18.7228	0.0033	9.4031	0.0048	4.2353	0.0072	5.1150	0.0065	3.5040	0.0080

**Table 4** Energy buildup factors for different spherical shields exposed to <sup>192</sup>Ir source with relative error

mfp(μr)	Al		Concrete		Fe		Sn		Pb		W		U	
	B <sub>E</sub>	Rel. Er	B <sub>E</sub>	Rel. Er	B <sub>E</sub>	Rel. Er	B <sub>E</sub>	Rel. Er	B <sub>E</sub>	Rel. Er	B <sub>E</sub>	Rel. Er	B <sub>E</sub>	Rel. Er
1	2.1291	0.0001	2.1286	0.0001	1.9206	0.0001	1.5438	0.0001	1.1693	0.0001	1.1516	0.0001	1.0616	0.0002
2	3.8836	0.0001	3.8822	0.0001	3.0920	0.0001	2.2287	0.0002	1.5145	0.0002	1.4453	0.0002	1.2735	0.0003
3	6.2875	0.0002	6.2817	0.0002	4.6060	0.0002	3.2351	0.0003	2.1792	0.0003	1.9987	0.0004	1.4081	0.0004
4	9.4539	0.0002	9.4387	0.0002	6.5877	0.0003	4.7784	0.0004	3.3398	0.0005	2.9319	0.0005	1.9769	0.0006
5	13.5583	0.0003	13.5335	0.0003	9.2037	0.0004	7.1794	0.0005	5.3058	0.0006	4.4463	0.0007	2.8783	0.0009
6	18.8563	0.0005	18.7937	0.0005	12.6891	0.0006	10.9402	0.0007	8.6012	0.0008	6.8628	0.0009	4.2851	0.0012
7	25.6429	0.0007	25.5711	0.0007	17.3300	0.0009	16.8127	0.0010	14.1169	0.0011	10.7203	0.0013	6.4886	0.0016
8	34.4228	0.0010	34.2652	0.0010	23.5599	0.0013	26.0001	0.0013	23.4614	0.0014	16.9312	0.0017	10.0046	0.0022
9	45.6195	0.0014	45.3119	0.0014	31.7990	0.0019	40.4034	0.0017	39.4000	0.0018	26.9972	0.0022	15.6735	0.0029
10	59.8547	0.0021	59.6359	0.0022	43.0185	0.0027	63.0749	0.0023	66.7777	0.0023	43.3596	0.0029	24.8800	0.0039

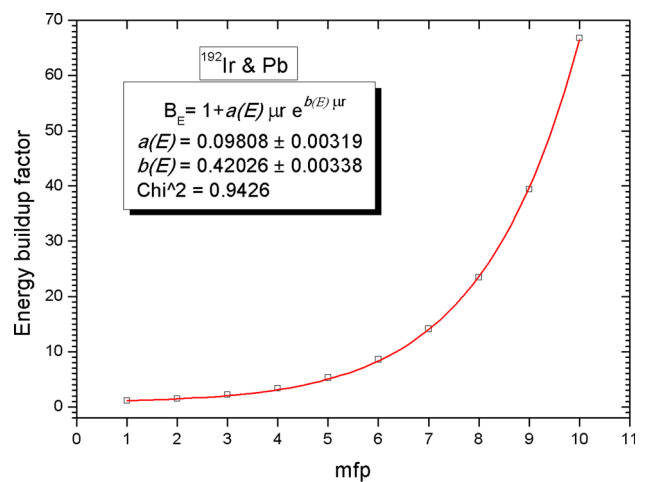
**Table 5** Energy buildup factors for different spherical shields exposed to <sup>75</sup>Se source with relative error

mfp(μr)	Al		Concrete		Fe		Sn		Pb		W		U	
	B <sub>E</sub>	Rel. Er	B <sub>E</sub>	Rel. Er	B <sub>E</sub>	Rel. Er	B <sub>E</sub>	Rel. Er	B <sub>E</sub>	Rel. Er	B <sub>E</sub>	Rel. Er	B <sub>E</sub>	Rel. Er
1	2.2519	0.0001	2.2510	0.0001	1.8651	0.0001	1.3352	0.0001	1.0784	0.0002	1.1231	0.0002	1.0501	0.0002
2	4.2912	0.0001	4.2862	0.0001	3.1886	0.0001	2.1342	0.0002	1.1771	0.0003	1.2772	0.0003	1.1554	0.0003
3	7.3182	0.0002	7.2996	0.0002	5.3159	0.0002	3.4701	0.0003	1.3127	0.0005	1.7593	0.0004	1.2001	0.0005
4	11.6973	0.0002	11.6378	0.0002	8.7214	0.0003	5.6688	0.0004	1.8136	0.0007	2.5587	0.0006	1.6278	0.0007
5	17.9389	0.0003	17.8077	0.0003	14.1145	0.0004	9.3340	0.0005	2.6912	0.0010	3.9260	0.0008	2.3893	0.0010
6	26.7678	0.0004	26.5023	0.0004	22.5640	0.0005	15.5484	0.0006	4.2063	0.0013	6.3194	0.0011	3.7063	0.0014
7	39.1848	0.0006	38.6950	0.0006	35.7440	0.0007	26.2618	0.0008	6.8126	0.0017	10.5198	0.0014	5.9609	0.0018
8	56.4641	0.0009	55.6294	0.0009	56.1843	0.0009	44.8854	0.0011	11.2570	0.0022	17.9859	0.0017	9.7780	0.0024
9	80.5345	0.0012	79.0683	0.0012	87.7491	0.0013	77.8297	0.0014	18.8703	0.0028	31.1673	0.0022	16.2542	0.0030
10	113.3858	0.0017	111.2897	0.0017	136.6147	0.0017	136.7750	0.0017	31.9182	0.0036	54.5957	0.0028	27.3065	0.0039

**Table 6** Energy buildup factors for different spherical shields exposed to <sup>169</sup>Yb source with relative error

mfp(μr)	Al		Concrete		Fe		Sn		Pb		W		U	
	B <sub>E</sub>	Rel. Er	B <sub>E</sub>	Rel. Er	B <sub>E</sub>	Rel. Er	B <sub>E</sub>	Rel. Er	B <sub>E</sub>	Rel. Er	B <sub>E</sub>	Rel. Er	B <sub>E</sub>	Rel. Er
1	2.2561	0.0001	2.2563	0.0001	1.7196	0.0001	1.1323	0.0002	1.1061	0.0002	1.1233	0.0002	1.0803	0.0002
2	4.5900	0.0001	4.5796	0.0001	3.1318	0.0002	1.6975	0.0003	1.1963	0.0003	1.2813	0.0003	1.1742	0.0004
3	8.7079	0.0002	8.6563	0.0002	5.5747	0.0002	2.7086	0.0004	1.5682	0.0005	1.5820	0.0005	1.2304	0.0006
4	15.7293	0.0002	15.5685	0.0002	9.8107	0.0003	4.5312	0.0005	2.5063	0.0007	2.5564	0.0007	1.6287	0.0008
5	27.4422	0.0003	27.0291	0.0003	17.1650	0.0004	7.8931	0.0006	4.2856	0.0008	4.4032	0.0008	2.5534	0.0011
6	46.6538	0.0004	45.7393	0.0004	29.9413	0.0005	14.2149	0.0008	7.6172	0.0011	7.8591	0.0010	4.1634	0.0014
7	77.8355	0.0005	75.8886	0.0005	52.1290	0.0006	26.2256	0.0009	13.8201	0.0013	14.2966	0.0013	6.8997	0.0018
8	127.9892	0.0006	124.1999	0.0006	90.7647	0.0008	49.0863	0.0012	25.3059	0.0016	26.2104	0.0016	11.4972	0.0024
9	208.2540	0.0008	201.0756	0.0009	158.4860	0.0010	93.0687	0.0014	46.5964	0.0019	48.3109	0.0019	19.2115	0.0030
10	335.9561	0.0011	322.7651	0.0011	276.5032	0.0013	177.7362	0.0017	85.7270	0.0024	89.1128	0.0023	32.3750	0.0039

**Fig. 9** A typical fitting plot representing the B<sub>E</sub> as a function of μr (Eq. (6)) for <sup>192</sup>Ir source inside the lead shield



Therefore, for each source of gamma-rays and the desired thickness of shield material, the energy buildup factor can be reproduced from Eq. (6) and presented coefficients in Table 7.

Validating the Monte Carlo simulations was performed with experiment. The linear attenuation coefficients were obtained through measurements with the CsI(Tl) γ-ray spectrometer, where they are listed and compared with the μ values calculated by Monte Carlo calculation in Table 8. It can be seen that the μ values calculated with MCNPX codes, shown in Table 1, are in agreement with the measured linear attenuation coefficients.



**Table 7** Coefficients of the Berger equation for energy buildup factors

	<sup>60</sup> Co		<sup>137</sup> Cs		<sup>192</sup> Ir		<sup>75</sup> Se		<sup>169</sup> Yb	
	<i>a</i>	<i>b</i>	<i>a</i>	<i>b</i>	<i>a</i>	<i>b</i>	<i>a</i>	<i>b</i>	<i>a</i>	<i>b</i>
Al	0.7936	0.0563	1.0766	0.0860	1.0630	0.1711	1.0162	0.2402	0.8437	0.3668
Conc	0.7923	0.0558	1.0778	0.0860	1.0602	0.1709	1.0226	0.2375	0.8510	0.3619
Fe	0.7152	0.0519	0.8684	0.0721	0.6207	0.1906	0.5028	0.3279	0.3959	0.4177
Sn	0.5607	0.0429	0.5712	0.0387	0.2188	0.3340	0.1890	0.4229	0.1113	0.4983
Pb	0.3632	0.0248	0.2950	0.0083	0.0981	0.4203	0.0376	0.4409	0.0504	0.5125
W	0.4123	0.0284	0.3538	0.0145	0.1021	0.3723	0.0544	0.4587	0.0517	0.5138
U	0.3039	0.0212	0.2413	0.0020	0.0564	0.3744	0.0322	0.4403	0.0377	0.4423

**Fig. 10** Comparison of energy buildup factors for <sup>192</sup>Ir obtained from Berger fitting and MCNPX calculations

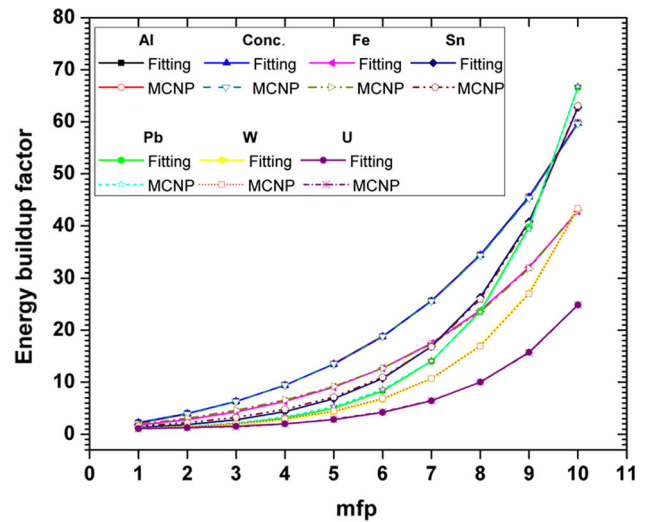


**Table 8** The measured  $\mu$  and relative difference with calculated value

	<sup>60</sup> Co		<sup>137</sup> Cs	
	$\mu_{exp}$ (cm) $\pm \Delta\mu$	$\frac{ \mu_{exp}-\mu_{cal} }{\mu_{exp}} \times 100$	$\mu_{exp}$ (cm) $\pm \Delta\mu$	$\frac{ \mu_{exp}-\mu_{cal} }{\mu_{exp}} \times 100$
Fe	0.425 $\pm$ 0.012	1.22	0.563 $\pm$ 0.017	2.65
Pb	0.651 $\pm$ 0.014	1.08	1.212 $\pm$ 0.011	1.40

The results of experiment for flux buildup factor of <sup>60</sup>Co and <sup>137</sup>Cs sources are arranged in Table 9, which includes uncertainty of each measurement, and percentage of relative differences in the experimental and computational results of this factor.

The relative differences between results of calculations and experiment are less than 4%, where it is reasonable and acceptable. The main Monte Carlo simulation error is statistical error, although the cross sections used in the calculation may also have errors. The significant error causes of the experiment are systematic errors, in which the uncertainty in activity of the source was more important.

### 4 Conclusions

The flux and energy buildup factors were calculated for different point isotropic sources used for industrial radiography (<sup>60</sup>Co, <sup>137</sup>Cs, <sup>192</sup>Ir, <sup>75</sup>Se and <sup>169</sup>Yb) placed in the center of seven shields, (Al, concrete, Fe, Sn, Pb, W and U) from 1 to 10 mfp using MCNPX code. The buildup factors are obtained very accurately by considering different interactions that are possible to occur between gamma photons and the medium matter with latest available cross section.

Buildup factor increases with increase in mean free path (material thickness) for the same gamma source. As thickness increases, the probability of photon scattering increases. For the same material thickness, the gamma sources with lower mean energy have larger buildup factor. For the photon in the range of 0.1 to 1.3 MeV, the cross section of Compton scattering reduces with increase in the energy. For the same gamma source and shield thickness, the materials with lower atomic number have greater buildup factor. This is because that the Compton scattering cross section almost decreases by increasing the atomic number. The values of buildup

**Table 9** The measured  $B_F$  and relative difference with calculated value

mfp ( $\mu\text{r}$ )	Fe		$^{60}\text{Co}$		$^{137}\text{Cs}$		Pb	
	$B_{F\text{-exp}}$	$\frac{ B_{F\text{-exp}} - B_{F\text{-cal}} }{B_{F\text{-exp}}} \times 100$	$B_{F\text{-exp}}$	$\frac{ B_{F\text{-exp}} - B_{F\text{-cal}} }{B_{F\text{-exp}}} \times 100$	$B_{F\text{-exp}}$	$\frac{ B_{F\text{-exp}} - B_{F\text{-cal}} }{B_{F\text{-exp}}} \times 100$	$B_{F\text{-exp}}$	$\frac{ B_{F\text{-exp}} - B_{F\text{-cal}} }{B_{F\text{-exp}}} \times 100$
3	$6.31 \pm 0.05$	2.46	$6.59 \pm 0.04$	2.24	$2.68 \pm 0.04$	2.20	$2.21 \pm 0.04$	1.29
5	$11.94 \pm 0.10$	3.79	$12.20 \pm 0.08$	3.35	$3.76 \pm 0.07$	3.31	$2.80 \pm 0.05$	3.20

factor for aluminum and concrete are close to each other. This may be due to the closeness of their effective atomic number. The results of experiment and Monte Carlo calculation for linear attenuation coefficient and flux buildup factor are in good agreement, as the relative differences are less than 3 and 4%, respectively. The outlined buildup factors of this study can be useful in applications of radiation shielding against gamma sources used for industrial radiography.

## References

1. IAEA, Radiation safety in industrial radiography: specific safety guide. International Atomic Energy Agency safety standards series, ISSN 1020–525X; no. SSG-11 (2011)
2. R. Halmshaw, *Industrial Radiology: Theory and Practice (English)* (Applied Science publishers Ltd., London and New Jersey, 1982)
3. IAEA-TECDOC-628/Rev.1, Training Guidelines in Non-destructive Testing Techniques, INIS Clearinghouse, International Atomic Energy Agency, Vienna (2008)
4. R.L. Heath, *Sintilation spectrometry gamma-ray spectrum catalogue*, 2nd ed. Idaho National Laboratory, Idaho (1997)
5. ISO 3999, Radiation Protection-Apparatus for Industrial Gamma Radiography-Specifications for Performance, Design and Tests, International Organization for Standardization, Geneva (2004)
6. NCRP 151, Structural shielding design and evaluation for megavoltage x- and gamma-ray radiotherapy facilities, National Council on Radiation Protection and Measurements, Bethesda (2005).
7. ICRP 103, The 2007 Recommendations of the International Commission on Radiological Protection (2007).
8. J.K. Shultis, R.E. Faw, *Radiation Shielding, La Grange Park* (American Nuclear Society, IL, 2000)
9. M.H. Alamatsaz, A. Shirani, Calculation of point isotropic buildup factors of gamma rays for water and lead. *Iran. J. Phy. Res.* **3**(1), 27–38 (2002)
10. G.R. White, The penetration and diffusion of cobalt-60 gamma-rays in water using spherical geometry. *Phys. Rev.* **80**, 154–156 (1950)
11. A.B. Chilton, J.K. Shultis, R.E. Faw, *Principle of Radiation Shielding*, vol. 189 (Prentice-Hall, Hoboken, 1984)
12. N. Tsoulfanidis, *Measurement and Detection of Radiation* (Taylor & Francis, London, 1995)
13. R. Khabaz, Specifying the flux and dose-equivalent buildup factors for infinite slabs irradiated by radionuclide neutron sources. *Appl. Radiat. Isot.* **157**, 109040 (2020)
14. N. Rostamani, R. Khabaz, Monte Carlo simulation estimates of absorbed dose in human organs due to the external exposure by decorative granite stones. *Radia. Phys. Chem.* **189**, 109702 (2021)
15. B. Pangh, R. Khabaz, A. Izadpanah, Measurement of outdoor and indoor ambient gamma dose rate in Gorgan and Bandar-Torkman cities using gas and thermoluminescent dosimeters. *Iran. J. Health Environ.* **12**(3), 397–408 (2019)
16. X. Li, W. Xiong, X. Hu, S. Sun, H. Li, X. Yang, Q. Zhang, M. Nibart, A. Albergel, S. Fang, An accurate and ultrafast method for estimating three-dimensional radiological dose rate fields from arbitrary atmospheric radionuclide distributions. *Atmos. Environ.* **199**, 143–154 (2019)
17. S. Fang, X. Li, N. Wu, J. Li, Y. Liu, N. Xue, H. Li, J. Liu, W. Xiong, Q. Zhang, A. Albergel, Fast evaluation of three-dimensional gamma dose rate fields on non-equispaced grids for complex atmospheric radionuclide distributions. *J. Environ. Radioact.* **222**, 106355 (2020)
18. H. Nakayama, D. Satoh, H. Nagai, H. Terada, Development of local-scale high-resolution atmospheric dispersion model using large-eddy simulation part 6: introduction of detailed dose calculation method. *J. Nucl. Sci. Technol.* **58**, 949–969 (2021)
19. S.M. Kulwinder, Measurement of exposure buildup factors: The influence of scattered photons on gamma-ray attenuation coefficients. *Nucl. Instrum. Methods A* **877**, 1–8 (2018)
20. Y. Harima, Historical review and current status of buildup factor calculations and applications. *Radia. Phys. Chem.* **41**, 631–672 (1993)
21. Y. Shirakawa, A build-up treatment for thickness gauging of steel plates based on gamma-ray transmission. *Appl. Radiat. Isot.* **53**, 581–586 (2000)
22. H. Goldstein, J.E. Wilkins Jr, *Calculations of the Penetrations of Gamma rays*, White Plains, NY: Nuclear Development Associates; NYO-3075 (1954)
23. R. Khabaz, A new approach to examine the exposure and dose buildup factors for multi-energy radioisotopic gamma sources with GP analytical expression. *Radia. Phys. Chem.* **151**, 53–58 (2018)
24. F. Mohammad Rafie, R. Khabaz, Evaluation of the radiation protection capabilities of some metal oxide glasses against radioisotopic gamma sources. *Iran. J. Phy. Res.* **20**(3), 557–565 (2020)
25. V.P. Singh, N.M. Badiger, Energy absorption buildup factors, exposure buildup factors and Kerma for optically stimulated luminescence materials and their tissue equivalence for radiation dosimetry. *Radia. Phys. Chem.* **104**, 61–67 (2014)
26. D. Sardari, A. Abbaspour, S. Baradaran, F. Babapour, Estimation of gamma- and X-ray photons buildup factor in soft tissue with Monte Carol method. *Appl. Radiat. Isot.* **67**, 1438–1440 (2009)
27. V.P. Singh, N.M. Badiger, Gamma-ray exposure build-up factor of some brick materials in state of Punjab. *J. Radioprot.* **48**(4), 511–526 (2012)
28. K. Shin, H. Hirayama, Calculation of gamma-ray buildup factors for two-layered shields made of water, concrete and iron and application of approximating formula. *Radia. Phys. Chem.* **61**, 583–584 (2011)
29. ICRU 10b, Physical aspects of irradiation. *Journal of the International Commission on Radiation Units and Measurements*, os6(1) (1964)
30. D.B. Pelowitz, MCNPX-A general Monte-Carlo N-particle transport code, Version 2.6, LANL Report, LA-CP-07-1473, Los Alamos (2008)
31. H.G. Hughes, Information on the MCPLIB02 Photon Library, Los Alamos National Laboratory (1996)
32. R.J. McConn Jr, C.J. Gesh, R.T.Pagh, R.A. Rucker, R.G. Williams III, Compendium of Material Composition Data for Radiation Transport Modeling, Customs and Border Protection and Domestic Nuclear Detection Office under U.S. Department of Energy Contract DE-AC05-76RL01830 (2011)
33. J. Zeb, W. Arshed, A. Rashid, P. Akhter, AI-SHIELDER calculates shielding thickness of Aluminum for any photon emitting radionuclide between 0.5 to 10 MeV, OECD Nuclear Energy Agency (NEA) France, IAEA1432, 21 (2010)
34. M.J. Berger, J.A. Doggett, Reflection and transmission of gamma radiation by barriers: semi-analytic Monte Carlo calculation. *J. Res. Nat. Bur. Stand.* **56**, 89–98 (1956)